THE JOURNAL OF BIOLOGICAL CHEMISTRY VOL. 289, NO. 19, pp. 13197–13205, May 9, 2014

The N-terminal Domain Modulates α-Amino-3-hydroxy-5-methyl-4-isoxazolepropionic acid (AMPA) Receptor Desensitization*

Received for publication, October 13, 2013, and in revised form, March 19, 2014 Published, JBC Papers in Press, March 20, 2014, DOI 10.1074/jbc.M113.526301

Tommi Möykkynen[1], **Sarah K. Coleman**[1], **Artur Semenov, and Kari Keinänen**[2]

From the Division of Biochemistry and Biotechnology, Department of Biosciences, University of Helsinki, 00014 Helsinki, Finland

Background: The function of the AMPA receptor N-terminal domain (NTD) is unknown.
Results: Deletion of the NTD leads to reduced desensitization and surface expression of GluA1–4 AMPA receptors.
Conclusion: The NTD has a strong influence on the function and biosynthetic maturation of AMPA receptors.
Significance: The NTD has the potential to mediate allosteric regulation of AMPA receptor signaling.

AMPA receptors are tetrameric glutamate-gated ion channels that mediate fast synaptic neurotransmission in mammalian brain. Their subunits contain a two-lobed N-terminal domain (NTD) that comprises over 40% of the mature polypeptide. The NTD is not obligatory for the assembly of tetrameric receptors, and its functional role is still unclear. By analyzing full-length and NTD-deleted GluA1–4 AMPA receptors expressed in HEK 293 cells, we found that the removal of the NTD leads to a significant reduction in receptor transport to the plasma membrane, a higher steady state-to-peak current ratio of glutamate responses, and strongly increased sensitivity to glutamate toxicity in cell culture. Further analyses showed that NTD-deleted receptors display both a slower onset of desensitization and a faster recovery from desensitization of agonist responses. Our results indicate that the NTD promotes the biosynthetic maturation of AMPA receptors and, for membrane-expressed channels, enhances the stability of the desensitized state. Moreover, these findings suggest that interactions of the NTD with extracellular/synaptic ligands may be able to fine-tune AMPA receptor-mediated responses, in analogy with the allosteric regulatory role demonstrated for the NTD of NMDA receptors.

AMPA receptors are tetrameric cation channels composed of homo- and heteromeric assemblies of GluA1–4 subunits (1–3). The extracellular part of the receptor subunits is composed of two bilobed domains: the N-terminal domain (NTD)[3] of ~400 amino acid residues and the ligand-binding domain (LBD), consisting of two separate, 120- to 150-residue segments, one situated between the NTD and the first transmembrane segment (M1) and the other following the second (M2) transmembrane segment. Although a key role for the LBD in controlling structural transitions of the transmembrane ion channel core in the center of the tetramer is well established, the functional role of the NTD has remained less understood. Sequence conservation between orthologs (*e.g.* 91% identity between the NTDs of human and goldfish subunits) and paralogs (*e.g.* 52–62% identity in human AMPA receptor subunits) are indicative of strong evolutionary constraints maintaining important, and at least partially subunit-specific, functions.

Crystal structures of separately expressed GluA1–4 NTDs (4–8) and of the GluA2 tetrameric channel (9) show that NTDs have a bilobed "Venus flytrap" structure and associate as parallel dimers via contacts involving both lobes. The dimeric structure is in agreement with findings that separately expressed NTDs, unlike LBDs, dimerize readily in solution (5, 10) and with the demonstrations of the importance of the NTD in the subclass-specific oligomerization of AMPA and kainate receptors (11, 12). In view of the relative size of the NTD, amounting to nearly half of the receptor polypeptide, and level of sequence conservation, it is surprising that truncated subunits lacking the entire NTD are capable of forming robust glutamate-gated channels (13–15). This excludes an obligatory role of the NTD in the assembly of homomeric AMPA receptors, but recent studies suggest that it has an important role in the formation of heteromeric receptors (16–18). Ligand-gated channel activity of NTD-deleted receptors is consistent with the semiautonomous status of NTDs, evident from inspection of the crystal structure of GluA2 tetramers (9). There, the NTDs are arranged as a distinct layer on top of the LBDs with little contact area between them. Consistent with earlier proposed assembly models (19–21), both the NTD and LBD layers have a dimer-of-dimers quaternary arrangement. An additional interesting feature is an unusual crossover at the NTD-LBD boundary that separates the subunits, which form an NTD dimer to different dimers in the LBD layer.

The NTD shows sequence similarity to bacterial periplasmic amino acid-binding proteins and to the agonist-binding domain of metabotropic glutamate and GABA receptors (22) and, like these, features a potential ligand-binding cleft, but its possible endogenous ligands are unknown. In native receptors, the NTD is likely to protrude far into the extracellular space,

* This study was supported by Academy of Finland grant 137596 (to K. K.), by the Sigrid Juselius Foundation (to K. K.), and by the Magnus Ehrnrooth Foundation (to T. M. and S. K. C.).
[1] Both authors contributed equally to this work.
[2] To whom correspondence should be addressed: Dept. of Biosciences, P.O.B. 56 (Viikinkaari 5), University of Helsinki, 00014 Helsinki, Finland. E-mail: kari.keinanen@helsinki.fi.
[3] The abbreviations used are: NTD, N-terminal domain; LBD, ligand-binding domain; LDH, lactate dehydrogenase; endo H, endo-β-*N*-acetylglucosaminidase H; PNGase F, peptide-*N*-(acetyl-β-glucosaminyl)-asparagine amidase; NBQX, 1,2,3,4-tetrahydro-6-nitro-2,3-dioxobenzo[f]quinoxaline-7-sulfonamide.

facilitating interactions with synaptic components, including those associated with the presynaptic membrane. Consistent with this, NTD-mediated interactions with N-cadherin (23, 24) and neuronal pentraxins (25) have been reported to regulate synaptic stability and receptor targeting, respectively. Whether the NTD plays any role in regulating the ion channel function of AMPA receptors via these interactions or by other mechanisms is unclear.

In this study, we examined the effects of NTD deletion on the surface expression and functional properties of homomeric AMPA receptor channels. We show that, for all four AMPA receptor subunits, deletion of the NTD leads to slower desensitization and faster recovery from desensitization of glutamate responses. As a result, the truncated channels give rise to higher steady-state currents and confer the cells with an increased sensitivity to glutamate toxicity. Furthermore, in the absence of the NTD, the receptors mature and reach the plasma membrane much less efficiently than the full-length receptors. These findings indicate that the NTD imposes significant constraints on the conformational transitions of the LBD-ion channel core and underscore the role of the NTD in the biosynthetic maturation of AMPA receptors.

EXPERIMENTAL PROCEDURES

Antibodies—For immunoblotting, rabbit anti-GluA1$_{CTD}$ (1:2000) and anti-GluA2$_L$/4 (1:1000) antisera (27), rabbit anti-GluA2/3 IgG (1 μg/ml, Millipore, catalog no. 07-598), and monoclonal anti-FLAG M1 (1 μg/ml, Sigma, catalog no. F-3040) and anti-GAPDH (anti-glycerladehyde-3-phosphate dehydrogenase, 0.02 μg/ml, Sigma, catalog no. G-8795) antibodies were used. The secondary antibodies were anti-mouse (1:3000) or anti-rabbit (1:3000) conjugated to horseradish peroxidase (GE Healthcare).

DNA Constructs—Expression plasmids encoding AMPA receptor subunits and mutants thereof were all constructed in pcDNA3.1 (Stratagene), and they all carried an N-terminal FLAG epitope and represented the flip isoform (26). Unless indicated otherwise , the GluA2 constructs represented the Q/R site unedited (Q) variant and had a long C-terminal tail. Constructs for expression of GluA1 (27) and GluA1ΔNTD (28) and GluA4 and GluA4ΔNTD (13) have been described previously. Full-length and NTD-deleted, unedited GluA2 constructs were generated by using PCR-based standard molecular biological techniques from the edited, long-tailed template described previously (29). Because of the very low surface expression of wild-type GluA3, an LBD point mutation, R461G (28), was introduced to the GluA3 and GluA3ΔNTD constructs. The N-terminal residues of the NTD-deleted subunits (ΔNTD) were as follows (numbering starting from Met-1 of the primary translation product): GluA1, 395; GluA2, 407; GluA3, 406; and GluA4, 403. The accuracy of all constructs was verified by restriction mapping and by sequencing through PCR-amplified regions.

Cell Culture and Transfections—HEK293 and COS7 cells were cultured in DMEM supplemented with 10% fetal calf serum and penicillin/streptomycin and transfected with the appropriate plasmids by using calcium phosphate coprecipitation, as described previously (30). For patch clamp experiments, pEGFP1-C1 (Clontech) was cotransfected for the visualization of transfected cells.

Whole Cell Patch Clamp Electrophysiology—Whole cell patch clamp recordings were made from GFP-positive HEK293 cells with an Axopatch 1B patch clamp amplifier and pClamp 10 software (Molecular Devices, Sunnyvale, CA) at a holding potential of −60 mV (31). After gigaseal formation and rupturing the membrane in the cell-attached configuration, the patched cell was lifted from the bottom of the dish to facilitate solution exchange. Electrodes were pulled from borosilicate glass capillaries (World Precision Instruments, Stevenage, UK) and had a resistance of 2–4 MΩ when filled with internal solution containing 140 mM CsCl, 2 mM $MgCl_2$, 10 mM EGTA, and 10 mM HEPES (pH adjusted to 7.2 with CsOH and osmolarity adjusted to 315 mosmol). Cells were continuously perfused with the recording solution containing 150 mM NaCl, 2.5 mM KCl, 2.5 mM $CaCl_2$, 1 mM $MgCl_2$, 10 mM glucose, and 10 mM HEPES (pH 7.4; 320 mosmol). L-glutamate (Sigma-Aldrich) and kainate (Tocris) were diluted to recording solution and applied to the cells using a piezo-driven applicator (Siskiyou piezo switcher, Siskiyou Corp., Grants Pass, OR). The speed of solution exchange was typically 0.4 ms as measured from the 10–90% rise time of liquid junction potential. Drug applications lasted for 1 s, except for the determination of the rate of recovery from desensitization, in which case two consecutive 100- to 200-ms glutamate applications were made with 10- to 600-ms time intervals. Recordings were made at the sampling rate of 5 kHz and low pass Bessel-filtered at 1 kHz. Each drug application was done twice, and traces were averaged for analysis. Data analysis was done using Clampfit 10.2 software (Molecular Devices) and Prism 3.0 software (GraphPad, San Diego, CA).

Cytotoxicity Assay and Microscopy—HEK293 cells were transfected and plated in 12-well plates at 3×10^5 cells and 1 μg of DNA/well. In some experiments, as indicated in the figure legends, NBQX (10 μM, Abcam Biochemicals) was added immediately following transfection and again 24 h later. The cells were cultured for 40 h following transfection. Thereafter, lactate dehydrogenase (LDH) release was measured by using a Pierce™ LDH cytotoxicity kit (catalog no. 88954) according to the recommendations of the manufacturer, with the following modification. After removing an aliquot of culture medium for the LDH activity assay, the remaining cultures were subjected to complete cell lysis by freezing and thawing to yield a sample for determination of the maximal (total) LDH activity. Cell death was quantified by calculating the ratio of LDH released during 40-h culture to the maximal LDH activity. Representative micrographs of HEK293 cultures were acquired via an EVOS digital inverted microscope (AMG, Invitrogen) under a bright field and a ×10 objective.

Immunofluorescence Microscopy—COS7 cells transfected for expression of GluA1 and GluA4 constructs were fixed, permeabilized with Triton X-100, and analyzed by immunofluorescence microscopy essentially as described before (27, 30).

Biochemical Analyses—Protein concentrations were measured by bicinchoninic acid assay (Uptima, Interchim, France) using bovine serum albumin as a standard. SDS-PAGE, immunoblotting, and cell surface biotinylation were carried out

essentially as described previously (27, 32). The glycosylation status of receptor subunits was analyzed by determining the accessibility of *N*-glycans to endo-β-*N*-acetylglucosaminidase H (endo H, New England Biolabs, catalog no. P0702) or peptide-*N*-(acetyl-β-glucosaminyl)-asparagine amidase (PNGase F, New England Biolabs, catalog no. P0704), performed according to the instructions of the enzyme manufacturer. The proteins of interest were immunoprecipitated, resuspended in 20 μl of 0.5% SDS, 1% β-mercaptoethanol, and heated at 100 °C for 10 min. For Endo H treatment, sodium citrate (0.5 M, 4 μl, G5 buffer of the manufacturer) was added, followed by endoglycosidase H (1000 units, 2 μl). For PNGase F treatment, sodium phosphate buffer (0.5 M, 4 μl, G7 buffer) and Nonidet P-40 (10%, 4 μl) were added, followed by PNGase F (500 units, 2 μl). After 1-h incubation at 37 °C, the samples were analyzed by SDS-PAGE and immunoblotting. For immunoblotting, Clarity™ Western ECL substrate (Bio-Rad, catalog no. 170-5061) was used. The ECL signal was detected and measured by using the Bio-Rad ChemiDoc XRS system and Quantity One software. The pixel density of the immunoreactive bands was obtained from the longest possible exposure prior to saturation of the signal. The relative surface expression level was calculated as the ratio of pixel density values of the immunoreactive bands representing the surface-exposed and total cell extract samples, respectively, normalized to the whole sample volume. Similarly, the relative total expression levels were calculated as the ratio of pixel densities of receptor bands and those of GAPDH, used as an internal standard, in the same cell extract samples.

Statistical Analysis—Data are presented as mean ± S.E., unless stated and described otherwise, where *n* is the number of independent experiments. For comparison between full-length receptor and NTD-deleted receptors, unpaired Student's *t* test was used. In addition, cytotoxicity data were initially examined by one-way analysis of variance followed by Dunnet's multiple comparison test to control (untransfected cells). The statistical significance of *p* values was ranked as follows: *, $p < 0.05$; **, $p < 0.01$; ***, $p < 0.001$. All statistical analyses were done with GraphPad Prism versions 3 and 4 (GraphPad Software Ltd).

RESULTS

Expression of NTD-deleted AMPA Receptors in HEK293 Cells—Homomeric GluA1–4 receptors were expressed in transiently transfected HEK293 cells both as full-length molecules and as NTD-deleted truncated receptors (Fig. 1*A*). All constructs had an N-terminal FLAG tag engineered between the signal peptide and the first encoded residue of the mature polypeptide. To enable electrophysiological analysis of GluA2, the unedited variant with glutamine at position 607 was used (33, 34). The GluA3 constructs harbored a point mutation, R461G, that strongly increases the otherwise very poor plasma membrane expression of GluA3 homomers (28). In immunoblot analyses, the full-length GluA1–4 subunits appeared as an ~100 kDa and the NTD-deleted versions as an ~55 kDa FLAG-immunoreactive species, in good agreement with the respective expected sizes. Notably, with all four subunits, the NTD-deleted variant was expressed at a significantly higher level than the corresponding full-length polypeptide (Fig. 1*B*).

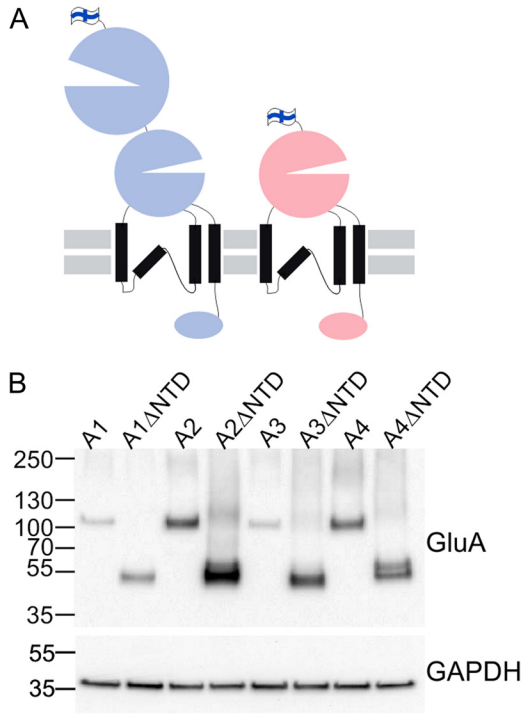

FIGURE 1. **Expression of the full-length and NTD-deleted AMPA receptors.** *A*, schematic of the full-length (*blue*) and NTD-deleted (*red*) subunits. All constructs used in the study have an extracellular, N-terminal FLAG tag fused just prior to the start of the AMPA receptor polypeptide. *B*, immunoblot analysis of transfected HEK293 cell extracts. Total protein loaded was 18 μg for all samples. *Top panel*, probed anti-FLAG IgG detecting the AMPA receptor proteins. *Bottom panel,* probed anti-GAPDH as a loading control. The NTD-deleted subunits show stronger expression than their corresponding full-length proteins.

Biosynthetic Maturation of NTD-deleted AMPA Receptors Is Impaired—To examine the effect of NTD deletion on receptor expression and maturation, we analyzed the total and surface-expressed levels of full-length and NTD-deleted GluA1–4 receptors in HEK293 cells. In a surface biotinylation assay, all receptor constructs were present on the plasma membrane, and the immunoreactivities of the full-length receptors were comparable with or slightly stronger than those of the truncated receptors, consistent with earlier findings (Ref. 28 and Fig. 2*A*, *top row*). However, in contrast to surface levels, the total expression levels of NTD-deleted receptors were consistently higher (Fig. 2*A*, *center row*). Quantitation of the intensities of the immunoreactive bands ($n = 4$ for all subunits), normalized to GAPDH in the same samples, showed that NTD-deleted GluA2–4 receptors were expressed at a roughly twice-higher level than the corresponding full-length receptors, whereas the difference was >10-fold for GluA1 (Fig. 2*C*). Under the experimental conditions used here, the plasma membrane expression levels of AMPA receptors are likely to reflect the efficiency of the forward trafficking of receptors from the endoplasmic reticulum to the cell surface (27). Calculated from the ratio of surface to total expression, the deletion of the NTD reduces the efficiency of receptor maturation by a factor of 2–8, depending on the subunit (Fig. 2*B*). With the exception of GluA3, the difference was statistically significant.

To further examine the role of the NTD in receptor maturation, we analyzed the subcellular localization and *N*-glycosyla-

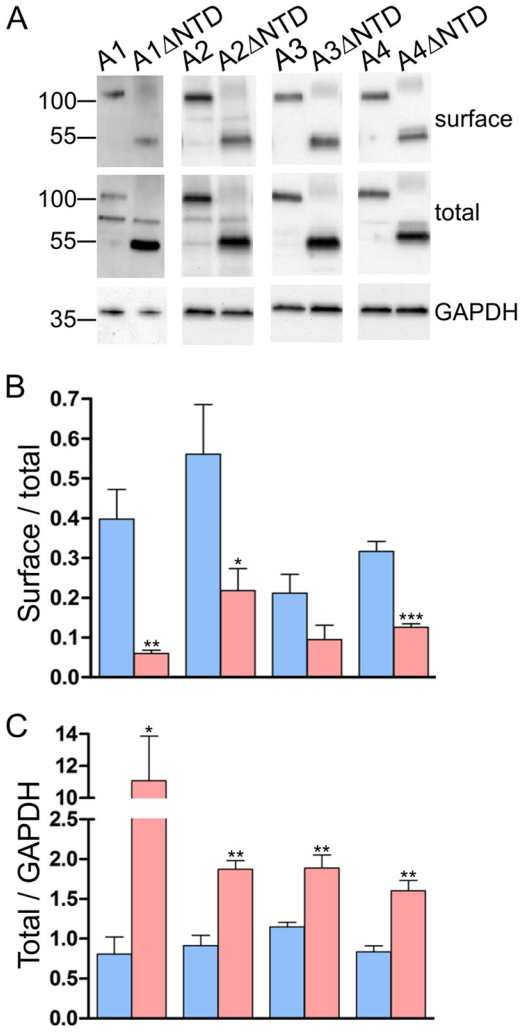

FIGURE 2. **Efficiency of surface expression of full-length and NTD-deleted AMPA receptors in transfected HEK293 cells.** *A*, immunoblot analyses showing the receptor levels on cell surface (*top row*) and in the total cell extract (*center row*). Plasma membrane expression was analyzed by using a surface biotinylation assay. The samples were probed by using the appropriate C-terminal domain-specific antibodies. *Bottom row*, GAPDH immunoreactivity in the same cell extracts, serving as a loading control and for signal normalization. Positions of molecular size markers are shown on the *left*. *B*, quantitation of relative surface expression levels. *, $p < 0.05$; **, $p < 0.01$; ***, $p < 0.001$. *C*, quantitation of relative total expression levels. **, $p < 0.01$. *B* and *C*, data are mean ± S.E. ($n = 4$) for the full-length and NTD-deleted receptors. The *bar graphs* correspond to the samples in *A*.

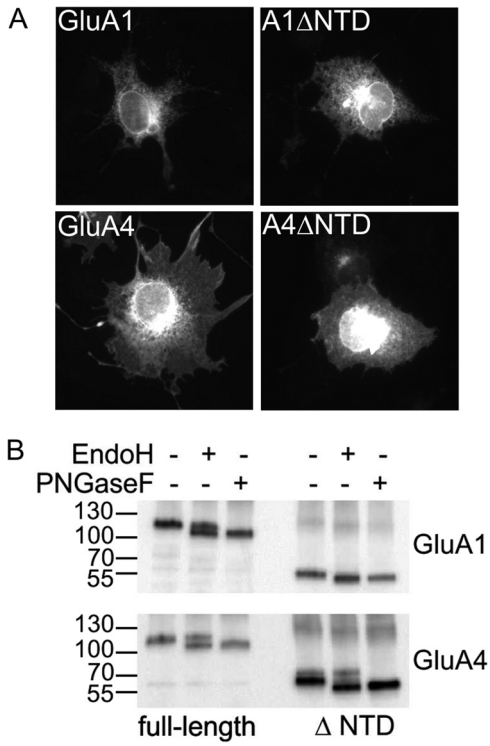

FIGURE 3. **Cellular distribution and glycosylation status of full-length and NTD-deleted GluA1 and GluA4 receptors.** *A*, representative micrographs showing the distribution of FLAG immunofluorescence in transfected COS7 cells. The staining was performed in fixed cells permeabilized with Triton X-100. *B*, immunoblot analysis showing the sensitivity of the glycosylated receptors to endoglycosidase H and PNGase F. Immunoprecipitated receptors were treated with enzymes as indicated at the top and analyzed by FLAG immunoblotting. Positions of molecular size markers are shown on the *left*.

tion of full-length and NTD-deleted GluA1 and GluA4 receptors expressed in COS7 cells. Immunofluorescence microscopy showed reticular cytoplasmic staining and strong perinuclear staining for all subunits, with no consistent subunit- or NTD-dependent differences (Fig. 3*A*). The accessibility of *N*-glycans to endo H and PNGase F was analyzed by immunoblotting of the enzyme-treated samples. PNGase F treatment completely converted both the full-length and NTD-deleted subunits to a faster-moving species, indicative of *N*-glycosylation. In contrast, a substantial fraction of the full-length receptors was resistant to endo H, whereas all (GluA1) or almost all (GluA4) of the NTD-deleted subunits were sensitive to endo H (Fig. 3*B*). Because resistance of N-glycans to endo H is acquired in the medial Golgi, the endo H-sensitive receptors are unlikely to have passed beyond cis-Golgi, consistent with defective endoplasmic reticulum exit. The glycosylation results are in good agreement with the surface expression data, including the more complete sensitivity of NTD-deleted GluA1 to endo H. Overall, the results indicate that deletion of the NTD leads to impaired maturation and accumulation in the endoplasmic reticulum.

NTD Deletion Reduces Desensitization of AMPA Receptors—We analyzed the currents evoked by glutamate application (10 mM, 1 s) in HEK293 cells expressing homomeric GluA1–4 receptors by using whole cell patch clamp recording at a holding potential of −60 mV. The current responses of all full-length and NTD-deleted receptors showed a distinct and rapidly decaying peak current followed by a steady-state current (Fig. 4*A*). The peak current amplitudes were typically between 2000–3500 pA and did not show consistent differences between the subunits or between the full-length and NTD-deleted receptors. Concentration-response curves determined for glutamate-induced peak currents did not show any significant difference between the full-length and NTD-deleted receptors (data not shown), consistent with previous findings on GluA4 (13). In contrast to the similar peak currents, all four NTD-deleted receptors produced significantly higher steady-state currents than the cognate full-length receptors. The effect was most pronounced in GluA1 (6.2-fold increase) and least prominent in GluA3 (2.6-fold increase) (Fig. 4*B*). Both an increased rate of onset of desensitization and a decreased rate of recovery from desensitization may contribute to the observed elevation of the steady state-to-peak current in NTD-deleted receptors.

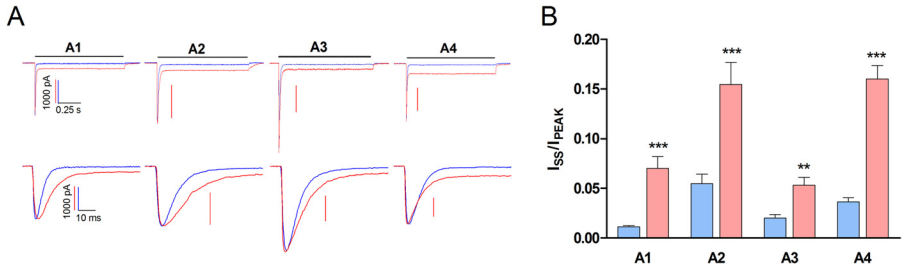

FIGURE 4. **Deletion of the NTD increases steady-state glutamate responses.** *A*, overlapping recording traces of 10 mM glutamate evoked currents of full-length (*blue*) and ΔNTD (*red*) GluA1-A4 AMPA receptors. The *black horizontal bar* indicates the glutamate application. The *scale bar* under the A1 trace applies to all full-length subunit receptors. The currents of ΔNTD receptors are scaled to the currents of wild types, and their amplitude is indicated by a *red vertical scale bar*. *Top row*, whole recordings. *Bottom row*, enlarged peak currents to illustrate the differences in the width of peak currents. *B*, the steady state/peak current ratios of full-length (*blue*) and ΔNTD (*red*) AMPA receptors. The number of independent measurements is 20 (A1), 16 (A1ΔNTD), 23 (A2), 11 (A2ΔNTD), 12 (A3), 15 (A3ΔNTD), 24 (A4), and 26 (A4ΔNTD). **, $p < 0.01$ ($p = 0.0024$), ***, $p < 0.001$, the difference between the full-length and ΔNTD.

We analyzed the desensitization kinetics in more detail. The time constants for onset of desensitization (τ_{des}) were calculated by fitting the decay of the peak current with a single exponential function. The deletion of the NTD caused a modest but significant (1.5- to 1.6-fold, $p > 0.001$) increase in τ_{des} in all subunits (Fig. 5*A*). The recovery from desensitization was analyzed by registering current responses to two successive glutamate pulses applied at variable time intervals (Fig. 5, *B–D*). Time constants (τ_{rec}) of the process were calculated from the time plots of the normalized peak current responses to the second glutamate application. Recovery from desensitization was significantly faster in the NTD-deleted receptors. The τ_{rec} value was approximately halved for all four receptor homomers (Fig. 5*B*). The robust effect of NTD deletion to resensitization kinetics of GluA1 homomers is illustrated in Fig. 5, *C* and *D*. For GluA1, τ_{rec} decreased from 154 ms (95% confidence interval, 147–160 ms) to 66.0 (62.2–70.3) ms (Fig. 5*B*). Thus, the higher steady-state-to-peak current ratio produced by NTD deletion reflects both a slower onset of desensitization and a faster recovery from desensitization, indicating that the desensitized state is less stable in the absence of the NTD.

Cells Expressing the NTD-deleted Receptor Show Enhanced Sensitivity to Glutamate Excitotoxicity—Upon microscopic inspection, we noticed that cultures transfected for expression of NTD-deleted receptors frequently had a slightly lower cell density and featured more floating cells than parallel cultures expressing full-length receptors. The finding that NTD-deleted receptors display higher steady-state responses to glutamate prompted us to test whether the enhanced cytotoxicity is caused by tonic activity caused by glutamate present in the culture medium, either released from dying cells or originating from glutamine or serum supplements of the culture medium. For this purpose, transfected cultures expressing full-length or NTD-deleted GluA1 and GluA2 receptors or selected control constructs were cultivated in the presence or absence of NBQX, a competitive AMPA receptor antagonist (35), and, 40 h post-transfection, cytotoxicity was quantified by using an LDH release assay. To control the effect of receptor protein expression independent of ion channel activity, the edited variant of GluA2, GluA2(R), was included. GluA2(R) channels are practically inactive but are highly expressed both as a full-length and NTD-deleted version (28). In addition, GluA4 carrying the "nondesensitizing" leucine-to-tyrosine mutation (L505Y (32, 36)) was used as a positive control. Cultures expressing full-length GluA1 (12.3 ± 0.90%, $n = 7$) or GluA2(R), either full-length (12.2 ± 0.92%, $n = 6$) or NTD-deleted (11.3 ± 0.77%, $n = 6$), showed the same level of LDH release as the nontransfected control cells (12.7 ± 0.70%, $n = 12$), indicating that transfection and expression of AMPA receptor polypeptides did not, in itself, affect cell viability (Fig. 6*A*). In contrast, GluA1ΔNTD transfectants (18.3 ± 1.4%, $n = 12$) and, very markedly, GluA2ΔNTD-expressing cells (42.5 ± 2.4%, $n = 12$) showed enhanced cytotoxicity, which was eliminated completely or mostly by NBQX (Fig. 6*A*). Notably, the detrimental effect of GluA2ΔNTD expression on cell viability was almost as high as that caused by expression of the nondesensitizing GluA4 L505Y mutant (48.9 ± 2.91%, $n = 8$). Slightly enhanced cytotoxicity (16.6 ± 1.5%, $n = 10$) was also seen in cultures expressing the full-length GluA2, consistent with its high steady current responses to glutamate (Fig. 4*B*). Cytotoxicity evaluated by LDH release assay correlated well to the visual appearance of the cultures under phase-contrast microscopy (Fig. 6*B*). These results indicate that the reduced desensitization caused by NTD deletion is reflected in live cells as enhanced sensitivity to toxicity caused by tonic glutamate activation.

Finally, to address the possibility that the impaired maturation of NTD-deleted receptors is caused by nonspecific effects related to cytotoxicity rather than intrinsic defects in the assembly and/or early transport of AMPA receptors, we studied the surface expression GluA2(R) receptors. Because of their poor conductance, the expression of GluA2(R) channels is not cytotoxic (see above). Quantitative analysis of surface and total expression, performed as described above under "Biosynthetic Maturation of NTD-deleted AMPA Receptors Is Impaired," showed that NTD-deleted GluA2(R) was expressed at a higher level than the full-length receptor but reached cell surface significantly less efficiently (Fig. 6*C*). The results are highly similar to those obtained with the (cytotoxic) GluA2(Q) and indicate that the poor maturation of NTD-deleted receptors is not due to their cytotoxic effect on the expressing cells.

DISCUSSION

Our analysis revealed that deletion of the N-terminal domain leads to significant changes in AMPA receptor function at two levels. First, the stead-state glutamate currents are strongly enhanced as a result of the slower onset of desensitization and faster recovery from desensitization. Second, the biosynthetic maturation occurs in a very inefficient manner. These findings

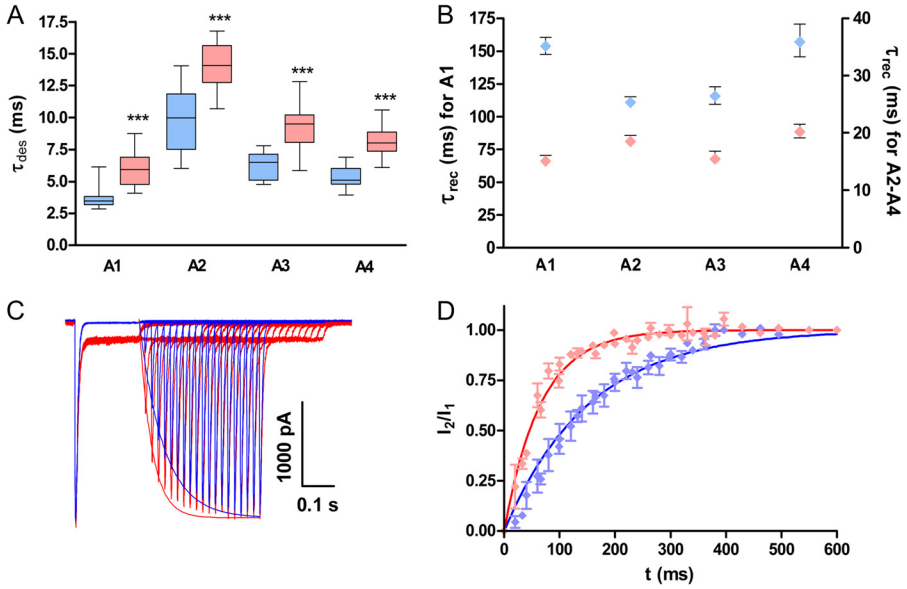

FIGURE 5. **The NTD modulates the desensitization kinetics of AMPA receptors.** *A*, τ values of desensitization measured from the decay of the peak current of full-length (*blue*) and ΔNTD (*red*) AMPA receptors. The *box* extends from the 25th percentile to the 75th percentile with a *line* at the medial (50th) percentile. The *whiskers* indicate the lowest and highest values. The numbers of independent measurements were 29 (A1), 20 (A1ΔNTD), 21 (A2), 12 (A2ΔNTD), 13 (A3), 15 (A3ΔNTD), 24 (A4), and 26 (A4ΔNTD). ***, $p < 0.001$, Student's *t* test. *B*, τ values of recovery from desensitization of A1-A4 full-length receptors (*light blue*) and ΔNTDs (*light red*). The *left y* axis is for A1 alone and the right is for A2-A4. *Error bars* indicate a 95% confidence interval ($n = 10–16$). The numbers of independent measurements were 10 (A1, A1ΔNTD, A2ΔNTD, and A4ΔNTD), 16 (A2 and A3), 13 (A3ΔNTD), and 11 (A4). *C*, overlapping recording traces of a single recovery from a desensitization experiment for full-length (*blue*) and ΔNTD (*red*) GluA1 AMPA receptors. The traces of ΔNTD are scaled to the same level as full-length receptors. *D*, curves of averaged recovery from desensitization experiments of the WT (*light blue*) and ΔNTD (*light red*) GluA1 subunit. Data are mean ± S.E. The *y* axis is the ratio of the amplitude of the second and first peak current.

have important implications for the understanding of AMPA receptor biogenesis and regulation.

Role of NTD in Desensitization—Rapid desensitization is one of the defining characteristics of AMPA receptor channels. It is thought to influence synaptic transmission, especially when glutamate uptake mechanisms are overloaded, as in the case of high-frequency stimulation or pathological (excitotoxic) situations (37, 38). According to the current model of desensitization of AMPA receptors, the glutamate-triggered gating motions build strain on the LBD dimer interface, which is disrupted as the receptor structure relaxes to a desensitized state with the channel closed (39, 40). The stability of the LBD dimer interface also plays a critical role in the desensitization of kainate receptors, although the detailed mechanisms may differ (41–44). The possible role of the NTD in desensitization has been overlooked because AMPA and kainate receptors also desensitize rapidly in the absence of the NTD (13, 19, 45). Our results indicate that, in all four homomeric AMPA receptor channels, NTD deletion retains glutamate-gated channel function but with significantly reduced desensitization. The latter is also reflected as clearly increased cytotoxicity of the expressed channels. We reported previously (13) that GluA4 channels lacking an NTD display slower desensitization (13), but the result was statistically less robust than in this study, probably because of a smaller number of independent measurements (5 *versus* 24–26 in this study). In addition to GluA4, slower desensitization of NTD-deleted GluA2 receptors has been noticed (15, 19). The reduced desensitization suggests that, in the native receptor, NTD imposes tension on the LBD ion channel core, which may add to the strain built on the LBD dimer interface upon receptor activation, and, thus, promotes LBD dimer dissociation (39, 44), as indicated in Fig. 7. The crystal structure of GluA2 tetramers or other available structural data do not lend themselves to any simple mechanistic explanation, but, in principle, the NTD can exert such an influence on the LBD channel core either via the NTD-LBD peptide linkers or through specific interdomain contacts. The structure of the GluA2-antagonist complex shows little interdomain interaction between the NTD and LBD layers, but it is possible that alternative conformations may exist that feature a more direct interaction between the domains. A role of NTD-LBD linkers is indirectly supported by the finding that the GluA2 construct engineered for crystallization ($GluA2_{cryst}$) displayed faster desensitization of glutamate responses than wild-type GluA2 (Ref. 9, supplemental Fig. 8). In $GluA2_{cryst}$, the NTD-LBD linker was modified by the deletion of six residues and elimination of two *N*-glycosylation sites, changes that are likely to change interdomain flexibility and possibly increase the tension imposed on the active conformation to promote desensitization.

Allosteric Potential of the NTD—The role of the NTD in the allosteric regulation of NMDA receptor channels by external Zn^{2+} ions, protons, and polyamines is well established (for a recent reviews, see Refs. 46, 47). At least some of this regulation may be mediated by ligand-induced closure of the NTD clamshell, which has been proposed to prevent or inhibit the closure of the LBD and, thus, to negatively influence ion channel function (48, 49). Alternatively, more subtle conformational changes, independent of cleft closure, may be involved (50). In fact, crystal structures of the Zn^{2+}-bound and free NTD of the GluN2B subunit indicate that the NTD also favors a closed conformation in the absence of Zn^{2+} ions (Ref. 51 but see 52). The quaternary organization of AMPA receptor NTDs

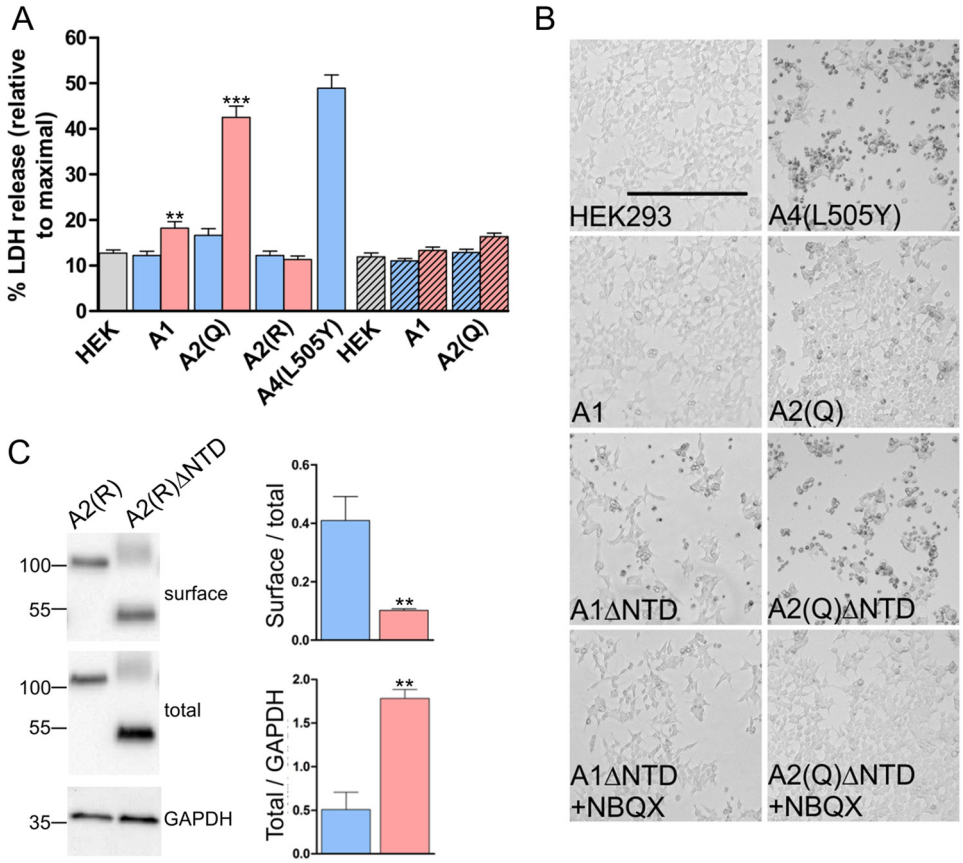

FIGURE 6. **NTD removal increases cytotoxicity.** *A*, quantification of cell death following transfection and expression of the indicated receptors. *Blue bars*, full-length receptors; *red bars*, NTD-deleted receptors; *HEK*, control cells incubated with transfection reagents but no DNA; *hatched bars*, presence of NBQX in the culture medium. *Error bars* indicate mean ± S.E. ($n = 6–12$). * ($p < 0.05$) and ** ($p < 0.01$) indicate the levels of significance in the statistical difference in LDH release between the NTD-deleted and its corresponding full-length receptors. The actual values are: GluA1, $p = 0.0074$; GluA2(Q), $p < 0.0001$; GluA2(R); $p = 0.473$. *B*, typical micrographs showing the effect on the cell population following the expression of the indicated receptors. *HEK293*, cells incubated with transfection reagents but no DNA. *Scale bar* = 400 μm. *C*, analysis of cell surface expression of GluA2(R) and GluA2(R)ΔNTD. The immunoblot analysis (*left panel*) shows the surface and total expression in a typical experiment, and the *bar graphs* (*right panel*) represent the quantitation of data from four experiments performed as in Fig. 2. **, $p < 0.01$.

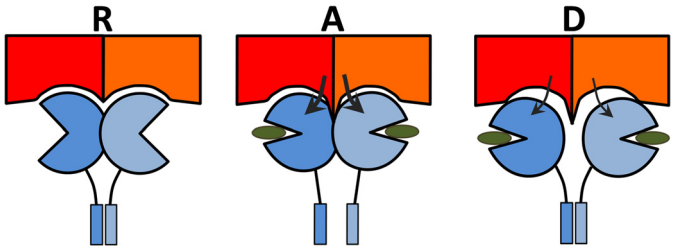

FIGURE 7. **The NTD regulates AMPA receptor desensitization.** Shown is a schematic illustrating the resting (*R*), active (*A*), and ligand-bound and desensitized (*D*) states of the AMPA receptor. Desensitization is depicted as a separation of LBD dimers. The NTD dimers exert force on the LBD to promote dimer separation (*arrows*). NTDs are *orange/red* shapes, LBDs are *blue circles*, membrane domains are *blue rectangles*, and ligands are *green ovals*.

differs from that in NMDA receptors, and a significant closure of the putative ligand-binding cleft in the AMPA receptor NTD is thought to be unlikely. AMPA receptor NTDs have, however, been shown to display flexibility (a prerequisite for an allosteric role), ranging from large-scale domain movements to more subtle conformational fluctuations (6, 8, 53–55). A wide range of NTD conformations, some differing substantially from the arrangement in $GluA2_{cryst}$, have been reported on the basis of electron microscopic (16, 53, 56–58) and atomic force microscopic (55) analyses of purified AMPA and kainate receptor preparations, supporting the view that the NTD can assume different conformations, at least under the specific experimental conditions used. Our findings suggest that protein or other ligand interactions that induce or stabilize specific NTD conformations that differ in their influence on the conformational freedom of the LBD channel core may facilitate the regulation of the strength and duration of AMPA receptor-mediated synaptic responses by the synaptic environment.

Role of NTD in Assembly and Maturation—The importance of the NTD in the subclass-specific assembly of ionotropic glutamate receptors (11, 12) and in the heteromeric assembly of AMPA (5, 18), kainate (17, 62) and NMDA receptors (59–61) has been established. Many studies have confirmed that NTD-driven dimerization is an important early step in the assembly (Refs. 16, 18, 59; for reviews, see Refs. 63–65), and point mutations in the NTD can lead to impaired maturation and surface expression (18, 59). Nascent receptor dimers held together by N-terminal dimerization and by transmembrane segment packing, but with clearly separate LBDs, have been identified in an electron microscopic analysis of AMPA receptor biosynthesis (16). The subsequent dimer-to-tetramer transition is thought to be driven by interdimer contacts forming between the transmembrane and NTD regions and to involve the

dimerization of LBDs across the original dimers (9, 16, 64, 65). From this scheme, it can be predicted that, in the absence of the NTD, the rates of initial dimerization and the subsequent dimer-to-tetramer transition would be affected severely. Our finding that NTD deletion leads to less efficient forward trafficking from the endoplasmic reticulum to the plasma membrane and, consequently, a reduced surface to total expression ratio, is consistent with the prediction. On the other hand, the absence of *N*-glycans present in the NTD may also contribute to the poor assembly and/or maturation of the truncated receptors. The functionality of NTD-deleted receptors indicates that, when formed, the tetramers are stable and able to undergo repeated cycles of activation and desensitization, including separation and reassociation of LBD dimers. At the same time, the present findings and earlier studies on NTD-deleted ionotropic glutamate receptors highlight the critical energetic contribution of the ion channel core to tetrameric assembly.

CONCLUSION

In conclusion, our study demonstrates that the N-terminal domain exerts a significant influence on AMPA receptor desensitization. These results raise the exciting possibility that this influence is regulated by interactions of the N-terminal domain with external proteins or other ligands.

REFERENCES

1. Palmer, C. L., Cotton, L., and Henley, J. M. (2005) The molecular pharmacology and cell biology of α-amino-3-hydroxy-5-methyl-4-isoxazolepropionic acid receptors. *Pharmacol. Rev.* **57,** 253–277
2. Collingridge, G. L., Olsen, R. W., Peters, J., and Spedding, M. (2009) A nomenclature for ligand-gated ion channels. *Neuropharmacology* **56,** 2–5
3. Traynelis, S. F., Wollmuth, L. P., McBain, C. J., Menniti, F. S., Vance, K. M., Ogden, K. K., Hansen, K. B., Yuan, H., Myers, S. J., and Dingledine, R. (2010) Glutamate receptor ion channels: structure, regulation, and function. *Pharmacol. Rev.* **62,** 405–496
4. Clayton, A., Siebold, C., Gilbert, R. J., Sutton, G. C., Harlos, K., McIlhinney, R. A., Jones, E. Y., and Aricescu, A. R. (2009) Crystal structure of the GluR2 amino-terminal domain provides insights into the architecture and assembly of ionotropic glutamate receptors. *J. Mol. Biol.* **392,** 1125–1132
5. Jin, R., Singh, S. K., Gu, S., Furukawa, H., Sobolevsky, A. I., Zhou, J., Jin, Y., and Gouaux, E. (2009) Crystal structure and association behaviour of the GluR2 amino-terminal domain. *EMBO J.* **28,** 1812–1823
6. Sukumaran, M., Rossmann, M., Shrivastava, I., Dutta, A., Bahar, I., and Greger, I. H. (2011) Dynamics and allosteric potential of the AMPA receptor N-terminal domain. *EMBO J.* **30,** 972–982
7. Yao, G., Zong, Y., Gu, S., Zhou, J., Xu, H., Mathews, I. I., and Jin, R. (2011) Crystal structure of the glutamate receptor GluA1 N-terminal domain. *Biochem. J.* **438,** 255–263
8. Dutta, A., Shrivastava, I. H., Sukumaran, M., Greger, I. H., and Bahar, I. (2012) Comparative dynamics of NMDA- and AMPA-glutamate receptor N-terminal domains. *Structure* **20,** 1838–1849
9. Sobolevsky, A. I., Rosconi, M. P., and Gouaux, E. (2009) X-ray structure, symmetry and mechanism of an AMPA-subtype glutamate receptor. *Nature* **462,** 745–756
10. Kuusinen, A., Abele, R., Madden, D. R., and Keinänen, K. (1999) Oligomerization and ligand-binding properties of the ectodomain of the α-amino-3-hydroxy-5-methyl-4-isoxazole propionic acid receptor subunit GluRD. *J. Biol. Chem.* **274,** 28937–28943
11. Leuschner, W. D., and Hoch, W. (1999) Subtype-specific assembly of α-amino-3-hydroxy-5-methyl-4-isoxazole propionic acid receptor subunits is mediated by their N-terminal domains. *J. Biol. Chem.* **274,** 16907–16916
12. Ayalon, G., and Stern-Bach, Y. (2001) Functional assembly of AMPA and kainate receptors is mediated by several discrete protein-protein interactions. *Neuron* **31,** 103–113
13. Pasternack, A., Coleman, S. K., Jouppila, A., Mottershead, D. G., Lindfors, M., Pasternack, M., and Keinänen, K. (2002) α-Amino-3-hydroxy-5-methyl-4-isoxazolepropionic acid (AMPA) receptor channels lacking the N-terminal domain. *J. Biol. Chem.* **277,** 49662–49667
14. Matsuda, S., Kamiya, Y., and Yuzaki, M. (2005) Roles of the N-terminal domain on the function and quaternary structure of the ionotropic glutamate receptor. *J. Biol. Chem.* **280,** 20021–20029
15. Bedoukian, M. A., Weeks, A. M., and Partin, K. M. (2006) Different domains of the AMPA receptor direct stargazin-mediated trafficking and stargazin-mediated modulation of kinetics. *J. Biol. Chem.* **281,** 23908–23921
16. Shanks, N. F., Maruo, T., Farina, A. N., Ellisman, M. H., and Nakagawa, T. (2010) Contribution of the global subunit structure and stargazin on the maturation of AMPA receptors. *J. Neurosci.* **30,** 2728–2740
17. Kumar, J., Schuck, P., and Mayer, M. L. (2011) Structure and assembly mechanism for heteromeric kainate receptors. *Neuron* **71,** 319–331
18. Rossmann, M., Sukumaran, M., Penn, A. C., Veprintsev, D. B., Babu, M. M., and Greger, I. H. (2011) Subunit-selective N-terminal domain associations organize the formation of AMPA receptor heteromers. *EMBO J.* **30,** 959–971
19. Horning, M. S., and Mayer, M. L. (2004) Regulation of AMPA receptor gating by ligand binding core dimers. *Neuron* **41,** 379–388
20. Tichelaar, W., Safferling, M., Keinänen, K., Stark, H., and Madden, D. R. (2004) The three-dimensional structure of an ionotropic glutamate receptor reveals a dimer-of-dimers assembly. *J. Mol. Biol.* **344,** 435–442
21. Sobolevsky, A. I., Yelshansky, M. V., and Wollmuth, L. P. (2004) The outer pore of the glutamate receptor channel has 2-fold rotational symmetry. *Neuron* **41,** 367–378
22. O'Hara, P. J., Sheppard, P. O., Thøgersen, H., Venezia, D., Haldeman, B. A., McGrane, V., Houamed, K. M., Thomsen, C., Gilbert, T. L., and Mulvihill, E. R. (1993) The ligand-binding domain in metabotropic glutamate receptors is related to bacterial periplasmic binding proteins. *Neuron* **11,** 41–52
23. Passafaro, M., Nakagawa, T., Sala, C., and Sheng, M. (2003) Induction of dendritic spines by an extracellular domain of AMPA receptor subunit GluR2. *Nature* **424,** 677–681
24. Saglietti, L., Dequidt, C., Kamieniarz, K., Rousset, M. C., Valnegri, P., Thoumine, O., Beretta, F., Fagni, L., Choquet, D., Sala, C., Sheng, M., and Passafaro, M. (2007) Extracellular interactions between GluR2 and N-cadherin in spine regulation. *Neuron* **54,** 461–477
25. Sia, G. M., Béïque, J. C., Rumbaugh, G., Cho, R., Worley, P. F., and Huganir, R. L. (2007) Interaction of the N-terminal domain of the AMPA receptor GluR4 subunit with the neuronal pentraxin NP1 mediates GluR4 synaptic recruitment. *Neuron* **55,** 87–102
26. Sommer, B., Keinänen, K., Verdoorn, T. A., Wisden, W., Burnashev, N., Herb, A., Köhler, M., Takagi, T., Sakmann, B., and Seeburg, P. H. (1990) Flip and flop: a cell-specific functional switch in glutamate-operated channels of the CNS. *Science* **249,** 1580–1585
27. Coleman, S. K., Möykkynen, T., Cai, C., von Ossowski, L., Kuismanen, E., Korpi, E. R., and Keinänen, K. (2006) Isoform-specific early trafficking of AMPA receptor flip and flop variants. *J. Neurosci.* **26,** 11220–11229
28. Coleman, S. K., Möykkynen, T., Hinkkuri, S., Vaahtera, L., Korpi, E. R., Pentikäinen, O. T., and Keinänen, K. (2010) Ligand-binding domain determines endoplasmic reticulum exit of AMPA receptors. *J. Biol. Chem.* **285,** 36032–36039
29. Coleman, S. K., Cai, C., Kalkkinen, N., Korpi, E. R., and Keinänen, K. (2010) Analysis of the potential role of GluA4 carboxyl-terminus in PDZ interactions. *PLoS ONE* **5,** e8715
30. Coleman, S. K., Cai, C., Mottershead, D. G., Haapalahti, J. P., and Keinänen, K. (2003) Surface expression of GluR-D AMPA receptor is dependent on an interaction between its C-terminal domain and a 4.1 protein. *J. Neurosci.* **23,** 798–806
31. Hamill, O. P., Marty, A., Neher, E., Sakmann, B., and Sigworth, F. J. (1981) Improved patch-clamp techniques for high-resolution current recording from cells and cell-free membrane patches. *Pflugers Arch.* **391,** 85–100
32. Coleman, S. K., Möykkynen, T., Jouppila, A., Koskelainen, S., Rivera, C., Korpi, E. R., and Keinänen, K. (2009) Agonist occupancy is essential for forward trafficking of AMPA receptors. *J. Neurosci.* **29,** 303–312
33. Sommer, B., Köhler, M., Sprengel, R., and Seeburg, P. H. (1991) RNA

editing in brain controls a determinant of ion flow in glutamate-gated channels. *Cell* **67,** 11–19
34. Swanson, G. T., Kamboj, S. K., and Cull-Candy, S. G. (1997) Single-channel properties of recombinant AMPA receptors depend on RNA editing, splice variation, and subunit composition. *J. Neurosci.* **17,** 58–69
35. Sheardown, M. J., Nielsen, E. O., Hansen, A. J., Jacobsen, P., and Honoré, T. (1990) 2,3-Dihydroxy-6-nitro-7-sulfamoyl-benzo(F)quinoxaline: a neuroprotectant for cerebral ischemia. *Science* **247,** 571–574
36. Stern-Bach, Y., Russo, S., Neuman, M., and Rosenmund, C. (1998) A point mutation in the glutamate binding site blocks desensitization of AMPA receptors. *Neuron* **21,** 907–918
37. Walker, C. S., Jensen, S., Ellison, M., Matta, J. A., Lee, W. Y., Imperial, J. S., Duclos, N., Brockie, P. J., Madsen, D. M., Isaac, J. T., Olivera, B., and Maricq, A. V. (2009) A novel *Conus* snail polypeptide causes excitotoxicity by blocking desensitization of AMPA receptors. *Curr. Biol.* **19,** 900–908
38. Christie, L. A., Russell, T. A., Xu, J., Wood, L., Shepherd, G. M., and Contractor, A. (2010) AMPA receptor desensitization mutation results in severe developmental phenotypes and early postnatal lethality. *Proc. Natl. Acad. Sci. U.S.A.* **107,** 9412–9417
39. Sun, Y., Olson, R., Horning, M., Armstrong, N., Mayer, M., and Gouaux, E. (2002) Mechanism of glutamate receptor desensitization. *Nature* **417,** 245–253
40. Armstrong, N., Jasti, J., Beich-Frandsen, M., and Gouaux, E. (2006) Measurement of conformational changes accompanying desensitization in an ionotropic glutamate receptor. *Cell* **127,** 85–97
41. Priel, A., Selak, S., Lerma, J., and Stern-Bach, Y. (2006) Block of kainate receptor desensitization uncovers a key trafficking checkpoint. *Neuron* **52,** 1037–1046
42. Weston, M. C., Schuck, P., Ghosal, A., Rosenmund, C., and Mayer, M. L. (2006) Conformational restriction blocks glutamate receptor desensitization. *Nat. Struct. Mol. Biol.* **13,** 1120–1127
43. Chaudhry, C., Plested, A. J., Schuck, P., and Mayer, M. L. (2009) Energetics of glutamate receptor ligand binding domain dimer assembly are modulated by allosteric ions. *Proc. Natl. Acad. Sci. U.S.A.* **106,** 12329–12334
44. Schauder, D. M., Kuybeda, O., Zhang, J., Klymko, K., Bartesaghi, A., Borgnia, M. J., Mayer, M. L., and Subramaniam, S. (2013) Glutamate receptor desensitization is mediated by changes in quaternary structure of the ligand binding domain. *Proc. Natl. Acad. Sci. U.S.A.* **110,** 5921–5926
45. Plested, A. J., and Mayer, M. L. (2007) Structure and mechanism of kainate receptor modulation by anions. *Neuron* **53,** 829–841
46. Paoletti, P., and Neyton, J. (2007) NMDA receptor subunits: function and pharmacology. *Curr. Opin. Pharmacol.* **7,** 39–47
47. Hansen, K. B., Furukawa, H., and Traynelis, S. F. (2010) Control of assembly and function of glutamate receptors by the amino-terminal domain. *Mol. Pharmacol.* **78,** 535–549
48. Gielen, M., Siegler Retchless, B., Mony, L., Johnson, J. W., and Paoletti, P. (2009) Mechanism of differential control of NMDA receptor activity by NR2 subunits. *Nature* **459,** 703–707
49. Yuan, H., Hansen, K. B., Vance, K. M., Ogden, K. K., and Traynelis, S. F. (2009) Control of NMDA receptor function by the NR2 subunit amino-terminal domain. *J. Neurosci.* **29,** 12045–12058
50. Zhu, S., Stroebel, D., Yao, C. A., Taly, A., and Paoletti, P. (2013) Allosteric signaling and dynamics of the clamshell-like NMDA receptor GluN1 N-terminal domain. *Nat. Struct. Mol. Biol.* **20,** 477–485
51. Karakas, E., Simorowski, N., and Furukawa, H. (2009) Structure of the zinc-bound amino-terminal domain of the NMDA receptor NR2B subunit. *EMBO J.* **28,** 3910–3920
52. Sirrieh, R. E., MacLean, D. M., and Jayaraman, V. (2013) Amino-terminal domain tetramer organization and structural effects of zinc binding in the *N*-methyl-D-aspartate (NMDA) receptor. *J. Biol. Chem.* **288,** 22555–22564
53. Nakagawa, T., Cheng, Y., Ramm, E., Sheng, M., and Walz, T. (2005) Structure and different conformational states of native AMPA receptor complexes. *Nature* **433,** 545–549
54. Jensen, M. H., Sukumaran, M., Johnson, C. M., Greger, I. H., and Neuweiler, H. (2011) Intrinsic motions in the N-terminal domain of an ionotropic glutamate receptor detected by fluorescence correlation spectroscopy. *J. Mol. Biol.* **414,** 96–105
55. Baranovic, J., Ramanujan, C. S., Kasai, N., Midgett, C. R., Madden, D. R., Torimitsu, K., and Ryan, J. F. (2013) Reconstitution of homomeric GluA2(flop) receptors in supported lipid membranes: functional and structural properties. *J. Biol. Chem.* **288,** 8647–8657
56. Nakagawa, T., Cheng, Y., Sheng, M., and Walz, T. (2006) Three-dimensional structure of an AMPA receptor without associated stargazin/TARP proteins. *Biol. Chem.* **387,** 179–187
57. Midgett, C. R., and Madden, D. R. (2008) The quaternary structure of a calcium-permeable AMPA receptor: conservation of shape and symmetry across functionally distinct subunit assemblies. *J. Mol. Biol.* **382,** 578–584
58. Midgett, C. R., Gill, A., and Madden, D. R. (2012) Domain architecture of a calcium-permeable AMPA receptor in a ligand-free conformation. *Front. Mol. Neurosci.* **4,** 56
59. Farina, A. N., Blain, K. Y., Maruo, T., Kwiatkowski, W., Choe, S., and Nakagawa, T. (2011) Separation of domain contacts is required for heterotetrameric assembly of functional NMDA receptors. *J. Neurosci.* **31,** 3565–3579
60. Karakas, E., Simorowski, N., and Furukawa, H. (2011) Subunit arrangement and phenylethanolamine binding in GluN1/GluN2B NMDA receptors. *Nature* **475,** 249–253
61. Lee, C. H., and Gouaux, E. (2011) Amino terminal domains of the NMDA receptor are organized as local heterodimers. *PLoS ONE* **6,** e19180
62. Kumar, J., Schuck, P., Jin, R., and Mayer, M. L. (2009) The N-terminal domain of GluR6-subtype glutamate receptor ion channels. *Nat. Struct. Mol. Biol.* **16,** 631–638
63. Greger, I. H., and Esteban, J. A. (2007) AMPA receptor biogenesis and trafficking. *Curr. Opin. Neurobiol.* **17,** 289–297
64. Nakagawa, T. (2010) The biochemistry, ultrastructure, and subunit assembly mechanism of AMPA receptors. *Mol. Neurobiol.* **42,** 161–184
65. Sukumaran, M., Penn, A. C., and Greger, I. H. (2012) AMPA receptor assembly: atomic determinants and built-in modulators. *Adv. Exp. Med. Biol.* **970,** 241–264